Alexandria Engineering Journal (2021) 60, 3345–3352

HOSTED BY

ELSEVIER

Alexandria University

Alexandria Engineering Journal

www.elsevier.com/locate/aej
www.sciencedirect.com

Turbulent energy motion of fiber suspensions in a rotating frame

S.F. Ahmed [a,*], M.G. Hafez [b], Yu-Ming Chu [c,*], M. Mofijur [d,e]

[a] *Science and Math Program, Asian University for Women, Chattogram 4000, Bangladesh*
[b] *Department of Mathematics, Chittagong University of Engineering and Technology, Chattogram 4349, Bangladesh*
[c] *Department of Mathematics, Huzhou University, Huzhou 313000, PR China*
[d] *School of Information, Systems and Modelling, Faculty of Engineering and Information Technology, University of Technology Sydney, Ultimo 2007, Australia*
[e] *Mechanical Engineering Department, Prince Mohammad Bin Fahad University, Al Khobar 31952, Saudi Arabia*

Received 12 August 2020; revised 21 January 2021; accepted 27 January 2021
Available online 15 February 2021

KEYWORDS

Turbulent flow;
Fiber suspension;
Rotating frame;
Correlation tensor;
Pressure–velocity correlation

Abstract Turbulent flows play a major role in many fields of science and industry. Noticeable attention is seen on turbulent flows of suspending fibers because of the sensitivity of the electrical, thermal, and mechanical properties of the connecting fiber composites to the spatial configuration and orientation of fibers. The involvement of fibers in the turbulent flow greatly affects the turbulent energy. It is more influenced when the turbulent flow occurs in a rotating system. The effect of fibers on the turbulent energy in the rotating frame must therefore be investigated. For turbulent energy with fiber suspension, a mathematical model can be built in a rotating system that is very important to enhance the quality of industrial goods. This paper, therefore, develops a mathematical model for turbulent energy motion in a rotating frame with a fiber suspension. The model was formulated using the averaging procedure. The momentum equation for incompressible and viscous fluid turbulent flow was considered to develop the model. The turbulent energy motion of the fiber suspensions was presented in the rotating frame in second-order correlation tensors, $W_{i,j}, S_{i,j}, L_{i,j}, F_{i,j}, G_{i,j}, D_{i,j}, Q_{i,j}$, and $H_{i,j}$, where all the tensors are the function of time, distance, and space coordinates.

1. Introduction

Rigorous theoretical investigations have been made on the turbulent flow due to its numerous applications. The applications are often seen in science, engineering, and industry, particularly in the ocean, nozzles and pipes, chemical mixers, the atmosphere, turbo-machinery, and combustion engines. It is occurred around the moving objects, e.g. different moving

* Corresponding authors.
E-mail addresses: shams.ahmed@auw.edu.bd (S.F. Ahmed), chuyuming@zjhu.edu.cn (Y.-M. Chu).

Peer review under responsibility of Faculty of Engineering, Alexandria University.

https://doi.org/10.1016/j.aej.2021.01.059
1110-0168

vehicles, influencing the resistance of flow to their bodies. Also, turbulence extends the energy required to propagate blood flow as turbulence may gain the energy loss for the case of friction like suspension of fibers in a turbulent flow.

The fluid flow behavior is described by turbulent motion that is based on fundamental laws of momentum, energy, and mass conservation. The equation of turbulent motion was derived by Hinze [1] in the second-order correlation, where the correlations were expressed in pressure–velocity and velocity fluctuations in the flow domain. But, the parameters that may affect the turbulent motion were not considered in his study to assess their impacts. A new mathematical model is therefore needs to be developed to overcome these issues and to conduct further research. The turbulent motion is significantly affected when fibers are injected into the flow. Suspension of fibers in turbulent flow is utilized in a greater portion of the industrial sector, especially in the papermaking, textile industry, chemical engineering, environmental engineering, producing composite materials, and so on. The fiber suspension property significantly affects the quality of products. Fiber suspensions into the turbulent flow also influence the light scattering, rheology, and transport properties of the suspensions. As a result, the turbulent flow along with fiber suspensions is becoming an incredible interest in several areas of industrial engineering.

For about the last thirty years, several researches [2–17] have been conducted on turbulent flow with fiber suspensions. Cho et al. [18] carried out preliminary research on turbulent fiber (ice crystals) motion. They discussed atmospheric turbulence and its impact on the orientation of fibers. The mean orientation of the fibers was not influenced substantially by atmospheric turbulence. Some other researches on fiber motion of turbulent flow involved glass fibers deposition in the human source tract [19,20]. Bernstein and Shapiro [21] assessed the lateral and axial orientation of fibers (glass) by considering different types of flow, namely laminar and turbulent flow. The axial distribution of fibers was observed wider close to the center of the pipe for the laminar flow, whereas nearly uniform distribution was found for the turbulent flow. Equations of motion of fluid flow were solved by Lin et al. [22] with a spectral approach, and fiber trajectories were calculated on the theory of the slender body. In their study, the Stokes number was found as a critical parameter for describing the spatial orientation of fibers on a large-scale. Its impact on fibers' orientation is trivial, and the fiber direction ratio has a minimal impact on fibers' orientation distribution. Fiber distribution was also simulated in a turbulent pipe flow [23]. The results showed that the distribution of fibers becomes broader with expanding Reynolds number (Re). The fibers' velocity fluctuation intensity was larger along the flow direction than that of cross direction whereas it was reverse for the fibers' angular velocity fluctuation intensity.

Kagermann and Koehler [24] examined the motion of non-spherical particles in turbulent flows. Noninteracting rigid spheroids were considered and suspended in homogeneous turbulent flows. The renormalized expansion was used in their study for the development of a kinetic equation with the Lagrangian correlation function of the turbulent velocity field and the orientational spheroid relaxation frequencies$\omega_u$and the coefficient of translational diffusion D. The moment method was applied to obtain the coupled integral relations of D andω_u. These were numerically solved for various energy spectrum correlation frequencies. The rotational and translational dispersion coefficients were found by Olson et al. [25], where the velocity between fluid and particles was ignored. Such dispersion coefficients of fiber were also obtained by Gao et al. [26] by balancing the virtual mass force and Stokes drag. They also analyzed the relationships between flow length scale and dispersion coefficients. Through these investigations, it is found that the particle length is increased while the dispersion coefficients are decreased. In most of the previous studies, the orientations of fibers were emphasized in turbulent flows. However, the turbulent properties of fiber suspensions were not considered or focused on those studies.

Lin et al. [27] proposed an equation for the fluid fluctuating velocity involving cylindrical particles in turbulent channel flow. They determined the Reynolds stress and fluid turbulent intensity by solving the equation with the mean of the fluctuating velocity. It was found that fibers play a key role in turbulent properties. However, the fluid impact on the suspended fibers was not considered in this study. Yang et al. [28] derived a two-way coupling model for turbulent flow to predict the additive-carrier flow field interaction. The probability distribution of fiber orientation was calculated using the Fokker-Plank equation. The impact of fiber concentration on rheological properties of suspended fibers and the distribution of fiber orientation were analyzed through numerical simulation. Numerical results demonstrated that a proper rise in concentration can enhance fiber alignment while the fiber concentration is near the semi-dilute phase. In other studies [29–31], only the experimental investigation was made to minimize the drag in turbulence with fiber suspensions.

Several studies [5,32–42] have been conducted in a rotating frame, particularly on the turbulent motion. Mahariq et al. [41] identified a nonlinear model for a flexible high aspect ratio with a free vibration response in a rotating system. The good accuracy was illustrated for the identified nonlinear model in contrasts between calculations and experiments. The average rotation prompts dynamical impacts on the turbulent flow that come into the transport equations over the pressure-strain-rate correlation [43]. In rotating turbulent flows, the rotation generates auxiliary body forces such as Coriolis and Centrifugal forces, following up on the turbulent structures, and thus the transfer mechanism of momentum is quite complex. However, most of the studies did not consider or discuss the impacts of system rotation with various angles due to the difficulties in the rotational frame.

Coriolis force performs a vital role in a rotating system for turbulent flow [44]. You et al. [36,45] made an experimental investigation to assess the Coriolis force impact on the turbulent flow in the rotating system. The authors considered particle image velocimetry (PIV) to quantify the flow field. The flow fields between the trailing and leading side were found different because of the Coriolis force effect [35]. The Coriolis force enlarged the vortex close to the leading side whereas it suppressed the vortex close to the trailing side. Coriolis force showed a noticeable impact on the vortices in the flow field. It was also demonstrated that not only the Coriolis force but also secondary flow affects the flow field which should not be ignored.

Through a literature survey, it is found that several sorts of research were presented on the laminar flow behavior of fiber suspensions because of the simplicity in the laminar flow. But, the turbulent flow behavior study of fiber suspensions are still inadequate owing to the complexity in turbulence and fiber motion. The flow behavior is abruptly changed and suffered from complexity if it occurs in a rotating frame. Due to the complexity and the difficulty level in mathematical modeling, no study has been undertaken on the turbulent energy of fiber suspensions in a rotating frame. Thus, this study is very important and timely for the industrial and engineering community. Therefore, this study aims to develop a model for the turbulent energy of fiber suspensions in a rotating frame. The resulting equation modeled by partial differential equations can be generalized for time–space fractional-order [46–49], and can therefore be useful to the broader scientific community. Due to the high accuracy, the spectral element method (SEM) [50–54] can be applied in solving the presently developed energy motion equation, and the SEM applications [55,56] are also recommended for further research.

2. Formulation of the model

The momentum equations of motion and the continuity for incompressible and viscous fluid turbulent flow are:

$$\frac{\partial u_i}{\partial t}+u_j\frac{\partial u_i}{\partial x_j}=-\frac{1}{\rho}\frac{\partial p}{\partial x_i}+\upsilon\frac{\partial^2 u_i}{\partial x_j\partial x_j}-2\varepsilon_{ijl}\Omega_j u_l \tag{1}$$

$$\frac{\partial u_i}{\partial x_i}=0 \tag{2}$$

In the case of fiber suspension in the flow field, the equation (1) becomes [3],

$$\frac{\partial u_i}{\partial t}+u_j\frac{\partial u_i}{\partial x_j}=-\frac{1}{\rho}\frac{\partial p}{\partial x_i}+\upsilon\frac{\partial^2 u_i}{\partial x_j\partial x_j}-2\varepsilon_{ijl}\Omega_j u_l+\frac{\mu_f}{\rho}\times\frac{\partial}{\partial x_j}\left[a_{ijlm}\varepsilon_{lm}-\frac{1}{3}\left(I_{ij}a_{lm}\right)\varepsilon_{lm}\right] \tag{3}$$

The following energy equation of motion is obtained for a rotating frame:

$$\frac{\partial u_i}{\partial t}+u_j\frac{\partial u_i}{\partial x_j}=-\frac{1}{\rho}\frac{\partial p}{\partial x_i}+\upsilon\frac{\partial^2 u_i}{\partial x_j\partial x_j}-2\varepsilon_{ijl}\Omega_j u_l-2(\Omega_i u_i\eta_i)\sin\theta \tag{4}$$

Therefore, the equation of turbulent energy motion for fiber suspensions in the rotating frame is given by

$$\frac{\partial u_i}{\partial t}+u_j\frac{\partial u_i}{\partial x_j}=-\frac{1}{\rho}\frac{\partial p}{\partial x_i}+\upsilon\frac{\partial^2 u_i}{\partial x_j\partial x_j}-2\varepsilon_{ijl}\Omega_j u_l+\frac{\mu_f}{\rho}\times\frac{\partial}{\partial x_j}\left[a_{ijlm}\varepsilon_{lm}-\frac{1}{3}\left(I_{ij}a_{lm}\right)\varepsilon_{lm}\right]-2(\Omega_i u_i\eta_i)\sin\theta \tag{5}$$

with the components of fluid velocity $u_i(x,t)$, pressure field $p(x,t)$, kinematical viscosity for the suspending fluid υ, fluid densityρ, permutation symbol ε_{ijl} (three-dimensional), turbulence dissipation ε (per unit mass), rotation vector Ω_j, $p=\frac{p}{\rho}+\frac{1}{2}\left|\bar{\Omega}\times\bar{u}\right|^2$indicates the generalized pressure consists of prospective centrifugal force, apparent viscosity for fiber suspensionsμ_f, tensor of strain rate $\varepsilon_{lm}=\frac{1}{2}\left(\frac{\partial u_l}{\partial x_m}+\frac{\partial u_m}{\partial x_l}\right)$, turbulent intensity for fiber suspensionsI_{ij}, second and fourth-order orientation tensors of fiber a_{lm} and a_{ijlm} respectively, $-2(\Omega_i u_i\eta_i)\sin\theta=-2\left(\bar{\Omega}\times\bar{u}\right)$ specifies the Coriolis force with the angular velocity Ω_i and the unit vector η normal to$\bar{u}$and$\bar{\Omega}$, θ is the measured angle between$\bar{u}$and $\bar{\Omega}$, and $t$is time.

Consider B and C are any points of the flow domain and suppose b & c are the given directions from the two points B and C respectively. Thus, u_b and u_c can be taken as the velocity components along with the directions B and C. Assume that $\bar{U}_i$is the average velocity which is constant all over the field considered and time-independent.

Therefore,

$$\left(U_i=\bar{U}_i+u_i\right)_B,\left(U_j=\bar{U}_j+u_j\right)_C$$

Each term has a value that can be determined by utilizing the equations for u_i at B point and for$u_j$at C point.

At point B, the energy equation can be expressed for$u_i$from Eq. (5),

$$\frac{\partial u_i}{\partial t}+\left(\bar{U}_k+u_k\right)\frac{\partial u_i}{\partial x_k}=-\frac{1}{\rho}\frac{\partial p}{\partial x_i}+\upsilon\frac{\partial^2 u_i}{\partial x_k\partial x_k}-2\varepsilon_{ikl}\Omega_k u_l-2(\Omega_i u_i\eta_i)\sin\theta+\frac{\mu_f}{\rho}\frac{\partial}{\partial x_k}\left[a_{iklm}\varepsilon_{lm}-\frac{1}{3}(I_{ik}a_{lm})\varepsilon_{lm}\right] \tag{6}$$

Since, $\left(u_i\frac{\partial u_k}{\partial x_k}\right)_B=0$ for an incompressible fluid, the Eq. (6) is derived as

$$\frac{\partial}{\partial t}(u_i)_B+\left[\bar{U}_k+(u_k)_B\right]\left(\frac{\partial}{\partial x_k}\right)_B(u_i)_B+\left(u_i\frac{\partial u_k}{\partial x_k}\right)_B=-\frac{1}{\rho}\left(\frac{\partial}{\partial x_i}\right)_B p_B+\upsilon\left(\frac{\partial^2}{\partial x_k\partial x_k}\right)_B(u_i)_B-2\left[(\varepsilon_{ikl}\Omega_k u_l)_B+(\Omega_i u_i\eta_i)_B\sin\theta\right]+\frac{\mu_f}{\rho}\left(\frac{\partial}{\partial x_k}\right)_B\left[a_{iklm}\varepsilon_{lm}-\frac{1}{3}(I_{ik}a_{lm})\varepsilon_{lm}\right]_B \tag{7}$$

Multiplying by$(u_j)_C$, the Eq. (7) gives

$$(u_j)_C\frac{\partial}{\partial t}(u_i)_B+\left[\bar{U}_k+(u_k)_B\right]\left(\frac{\partial}{\partial x_k}\right)_B(u_i)_B(u_j)_C+(u_i)_B\left(\frac{\partial}{\partial x_k}\right)_B(u_k)_B(u_j)_C=-\frac{1}{\rho}\left(\frac{\partial}{\partial x_i}\right)_B p_B(u_j)_C+\upsilon\left(\frac{\partial^2}{\partial x_k\partial x_k}\right)_B(u_i)_B(u_j)_C-2\left[(\varepsilon_{ikl}\Omega_k u_l)_B+(\Omega_i u_i\eta_i)_B\sin\theta\right](u_j)_C+\frac{\mu_f}{\rho}\left(\frac{\partial}{\partial x_k}\right)_B\left[a_{iklm}\varepsilon_{lm}-\frac{1}{3}(I_{ik}a_{lm})\varepsilon_{lm}\right]_B(u_j)_C \tag{8}$$

where $(u_j)_C$ is considered as constant at point B for a differential approach.

Similarly, for $u_j$the energy equation is obtained at point C:

$$\frac{\partial u_j}{\partial t}+\left(\bar{U}_k+u_k\right)\frac{\partial u_j}{\partial x_k}=-\frac{1}{\rho}\frac{\partial p}{\partial x_j}+\upsilon\frac{\partial^2 u_j}{\partial x_k\partial x_k}-2\varepsilon_{jkl}\Omega_k u_l-2(\Omega_j u_j\eta_j)\sin\theta+\frac{\mu_f}{\rho}\frac{\partial}{\partial x_k}\left[a_{jklm}\varepsilon_{lm}-\frac{1}{3}\left(I_{jk}a_{lm}\right)\varepsilon_{lm}\right] \tag{9}$$

By adopting the condition, $\left(u_j \frac{\partial u_k}{\partial x_k}\right)_C = 0$for an incompressible fluid, Eq. (9) yields

$$\frac{\partial}{\partial t}(u_j)_C + \left[\overline{U}_k + (u_k)_C\right]\left(\frac{\partial}{\partial x_k}\right)_C (u_j)_C + \left(u_j \frac{\partial u_k}{\partial x_k}\right)_C$$
$$= -\frac{1}{\rho}\left(\frac{\partial}{\partial x_j}\right)_C p_C + \upsilon\left(\frac{\partial^2}{\partial x_k \partial x_k}\right)_C (u_j)_C$$
$$-2\left[(\varepsilon_{jkl}\Omega_k u_l)_C + (\Omega_j u_j \eta_j)_C \sin\theta\right]$$
$$+\frac{\mu_f}{\rho}\left(\frac{\partial}{\partial x_k}\right)_C \left[a_{jklm}\varepsilon_{lm} - \frac{1}{3}(I_{jk}a_{lm})\varepsilon_{lm}\right]_C \tag{10}$$

The Eq. (10) is expressed as the following by multiplying$(u_i)_B$:

$$(u_i)_B \frac{\partial}{\partial t}(u_j)_C + \left[\overline{U}_k + (u_k)_C\right]\left(\frac{\partial}{\partial x_k}\right)_C (u_j)_C (u_i)_B$$
$$+ (u_j)_C \left(\frac{\partial}{\partial x_k}\right)_C (u_k)_C (u_i)_B$$

$$= -\frac{1}{\rho}\left(\frac{\partial}{\partial x_j}\right)_C p_C (u_i)_B + \upsilon\left(\frac{\partial^2}{\partial x_k \partial x_k}\right)_C (u_j)_C (u_i)_B$$
$$-2\left[(\varepsilon_{jkl}\Omega_k u_l)_C + (\Omega_j u_j \eta_j)_C \sin\theta\right](u_i)_B$$

$$+\frac{\mu_f}{\rho}\left(\frac{\partial}{\partial x_k}\right)_C \left[a_{jklm}\varepsilon_{lm} - \frac{1}{3}(I_{jk}a_{lm})\varepsilon_{lm}\right]_C (u_i)_B \tag{11}$$

where $(u_i)_B$ are considered as constants in differential approach at C point.

Adding the Eqs. (8) and (11),

$$\frac{\partial}{\partial t}(u_i)_B (u_j)_C$$
$$+\left[\left(\frac{\partial}{\partial x_k}\right)_B (u_i)_B (u_k)_B (u_j)_C + \left(\frac{\partial}{\partial x_k}\right)_C (u_i)_B (u_k)_C (u_j)_C\right]$$
$$+\overline{U}_k\left[\left(\frac{\partial}{\partial x_k}\right)_B (u_i)_B (u_j)_C + \left(\frac{\partial}{\partial x_k}\right)_C (u_i)_B (u_j)_C\right]$$

$$= -\frac{1}{\rho}\left[\left(\frac{\partial}{\partial x_i}\right)_B p_B (u_j)_C + \left(\frac{\partial}{\partial x_j}\right)_C p_B (u_i)_B\right]$$
$$+\upsilon\left[\left(\frac{\partial^2}{\partial x_k \partial x_k}\right)_B + \left(\frac{\partial^2}{\partial x_k \partial x_k}\right)_C\right](u_i)_B (u_j)_C$$

$$-2\left[(\varepsilon_{ikl}\Omega_k u_l)_B (u_j)_C + (\varepsilon_{jkl}\Omega_k u_l)_C (u_i)_B\right]$$
$$-2\left[(\Omega_i u_i \eta_i)_B (u_j)_C + (\Omega_j u_j \eta_j)_C (u_i)_B\right]\sin\theta$$

$$+\frac{\mu_f}{\rho}\left[\left(\frac{\partial}{\partial x_k}\right)_B \left(a_{iklm}\varepsilon_{lm} - \frac{1}{3}I_{ik}a_{lm}\varepsilon_{lm}\right)_B (u_j)_C\right.$$
$$\left.+\left(\frac{\partial}{\partial x_k}\right)_C \left(a_{jklm}\varepsilon_{lm} - \frac{1}{3}I_{jk}a_{lm}\varepsilon_{lm}\right)_C (u_i)_B\right] \tag{12}$$

To address turbulent energy relations at C toward those at B point, it will not make any differences if any of the points of B and C is considered as the origin for the coordinate system. Point B has been taken here as the origin. The independent variables, $\tau_k$have been chosen to distinguish the impacts between location and distance,

$\tau_k = (x_k)_C - (x_k)_B$

Thus, the followings are obtained,

$$\left(\frac{\partial}{\partial x_k}\right)_B = -\frac{\partial}{\partial \tau_k}, \left(\frac{\partial}{\partial x_k}\right)_C = \frac{\partial}{\partial \tau_k}$$

$$\left(\frac{\partial^2}{\partial x_k \partial x_k}\right)_B = \left(\frac{\partial^2}{\partial x_k \partial x_k}\right)_C = \frac{\partial^2}{\partial \tau_k \partial \tau_k}$$

Substituting the above expressions in Eq. (12) and taking the average to all of the terms, Eq. (12) becomes

$$\frac{\partial}{\partial t}\overline{(u_i)_B (u_j)_C} - \frac{\partial}{\partial \tau_k}\overline{(u_i)_B (u_k)_B (u_j)_C} + \frac{\partial}{\partial \tau_k}\overline{(u_i)_B (u_k)_C (u_j)_C}$$
$$= -\frac{1}{\rho}\left[-\frac{\partial}{\partial \tau_i}\overline{p_B (u_j)_C} + \frac{\partial}{\partial \tau_j}\overline{p_C (u_i)_B}\right]$$

$$+2\upsilon\frac{\partial^2}{\partial \tau_k \partial \tau_k}\overline{(u_i)_B (u_j)_C} - 2\left[\overline{(\varepsilon_{ikl}\Omega_k u_l)_B (u_j)_C} + \overline{(\varepsilon_{jkl}\Omega_k u_l)_C (u_i)_B}\right]$$
$$-2\left[\overline{(\Omega_i u_i \eta_i)_B (u_j)_C} + \overline{(\Omega_j u_j \eta_j)_C (u_i)_B}\right]\sin\theta$$

$$-\frac{\mu_f}{\rho}\frac{\partial}{\partial \tau_k}\left[\overline{(a_{iklm}\varepsilon_{lm})_B (u_j)_C} - \frac{1}{3}\overline{(I_{ik}a_{lm}\varepsilon_{lm})_B (u_j)_C} - \overline{(a_{jklm}\varepsilon_{lm})_C (u_i)_B}\right.$$
$$\left.+\frac{1}{3}\overline{(I_{jk}a_{lm}\varepsilon_{lm})_C (u_i)_B}\right] \tag{13}$$

Eq. (13) gives the average motion of turbulent energy for the suspension of fibers in the rotating system, where the turbulent fiber motions move with the average velocity, $\overline{U}_k$ as regards to a coordinate system. The coefficient term of $\overline{U}_k$ was vanished because of its constant-derivative.

The Eq. (13) consists of the double-velocity correlations $\overline{(u_i)_B (u_j)_C}$, double-pressure–velocity correlations $\overline{p_B (u_j)_C}$, triple-velocity correlations, for example, $\overline{(u_i)_B (u_k)_B (u_j)_C}$, where all of these terms are at a distance from one to another. The pressure–velocity correlations, $\overline{p_C (u_i)_B}$ and $\overline{p_C (u_j)_B}$ make first-order tensors, since the pressure is considered as a scalar quantity. Similarly, the triple-velocity correlations, $\overline{(u_i)_B (u_k)_C (u_j)_C}$, and $\overline{(u_i)_B (u_k)_B (u_j)_C}$form third-order tensors. In the flow field, the double triple pressure–velocity and velocity correlations at the points B and C are illustrated in Fig. 1(a, b) and Fig. 2 separately, where d is the gap between the points B and C.

The first-order, second-order, and third-order correlations can be designated by$(K_{p,j})_{B,C}$, $(W_{i,j})_{B,C}$, and$(S_{ik,j})_{B,C}$ respectively.

Therefore, the velocity correlations and pressure–velocity correlations become

$(K_{i,p})_{B,C} = \overline{(u_i)_B p_C}$, $(k_{p,j})_{B,C} = \overline{p_B (u_j)_C}$ $(W_{i,j})_{B,C} = \overline{(u_i)_B (u_j)_C}$

$(S_{ik,j})_{B,C} = \overline{(u_i)_B (u_k)_B (u_j)_C}$,and$(S_{i,kj})_{B,C} = \overline{(u_i)_B (u_k)_C (u_j)_C}$.

where$p$specifies the pressure that is an index not like the dummy$i$or$j$, and thus the summation must not be applied to$p$.

The terms$\overline{(\varepsilon_{jkl}\Omega_k u_l)_C (u_i)_B}$,$\overline{(\varepsilon_{ikl}\Omega_k u_l)_B (u_j)_C}$,$\overline{(\Omega_i u_i \eta_i)_B (u_j)_C}$, and $\overline{(\Omega_j u_j \eta_j)_C (u_i)_B}$form second-order correlation tensors which can be denoted by $M_{i,j}$, $N_{i,j}$, $F_{i,j}$, and$G_{i,j}$respectively whereas the terms $\overline{(I_{jk}a_{lm}\varepsilon_{lm})_C (u_i)_B}and\overline{(a_{jklm}\varepsilon_{lm})_C (u_i)_B}$form third-order correlation tensors, those can be represented by $H_{i,jk}$

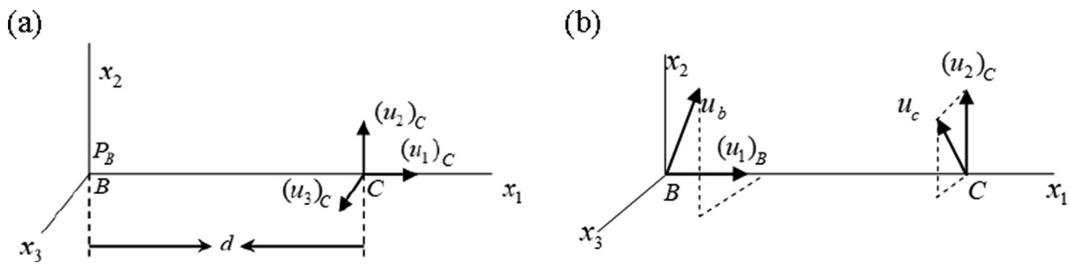

Fig. 1 Double correlations between points B and C. (a) Pressure at B and velocity at C. (b) Velocities $u_b$at B and $u_c$at C.

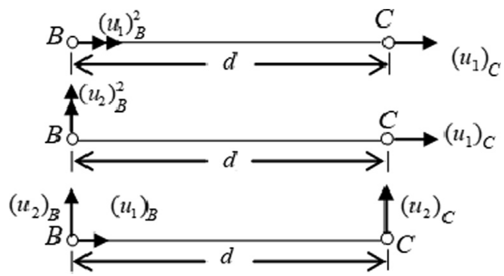

Fig. 2 Triple velocity correlation at B and C.

and$D_{i,jk}$respectively. Thus, the following expressions are obtained:

$$(M_{i,j})_{B,C} = \overline{(\varepsilon_{ikl}\Omega_k u_l)_B (u_j)_C}\,(N_{i,j})_{B,C} = \overline{(\varepsilon_{jkl}\Omega_k u_l)_C (u_i)_B}\,(D_{i,jk})_{B,C} = \overline{(u_i)_B (a_{jklm}\varepsilon_{lm})_C},$$

$$(D_{ik,j})_{B,C} = \overline{(a_{iklm}\varepsilon_{lm})_B (u_j)_C}\,(F_{i,j})_{B,C} = \overline{(\Omega_i u_i \eta_i)_B (u_j)_C}\,(G_{i,j})_{B,C} = \overline{(\Omega_j u_j \eta_j)_C (u_i)_B}$$

$$(H_{i,jk})_{B,C} = \overline{(u_i)_B (I_{jk} a_{lm}\varepsilon_{lm})_C},\ (H_{ik,j})_{B,C} = \overline{(I_{ik} a_{lm}\varepsilon_{lm})_B (u_j)_C}.$$

Substituting the above expressions of the correlations, Eq. (14) yields

$$\frac{\partial}{\partial t} W_{i,j} - \frac{\partial}{\partial \tau_k} S_{ik,j} + \frac{\partial}{\partial \tau_k} S_{i,kj} = -\frac{1}{\rho}\left(-\frac{\partial}{\partial \tau_i} K_{p,j} + \frac{\partial}{\partial \tau_j} K_{i,p}\right) + 2\upsilon \frac{\partial^2}{\partial \tau_k \partial \tau_k} W_{i,j} - 2\left[(M_{i,j} + N_{i,j})\right]$$

$$-2(F_{i,j} + G_{i,j})\sin\theta + \frac{\mu_f}{\rho} \times \frac{\partial}{\partial \tau_k}\left[(D_{i,jk} - D_{ik,j}) + \frac{1}{3}(H_{ik,j} - H_{i,jk})\right] \tag{14}$$

where the correlations in Eq. (14) concerning the measured points, B and C.

For an incompressible flow and isotropic turbulence, the double correlations of pressure–velocity must be zero, that means,

$$(k_{p,j})_{B,C} = 0,\ (k_{i,p})_{B,C} = 0$$

The statistical properties have no specific directional preference for the isotropy. The fluctuations in velocity are independent regards to the reference axis, that is, invariant to reflection and rotation of the axis. According to the isotropic definition, $(W_{i,j})_{B,C} = \overline{(u_i)_B (u_j)_C} = 0$ for every $i \neq j$. In a rotational system through the angle 180^0 about the x_1-axis must give the following due to the isotropy:

$$\overline{(u_1)_B (u_2)_C} = \overline{(u_1)_B [-(u_2)]_C} = -\overline{(u_1)_B (u_2)_C}$$

which will be true while $\overline{(u_1)_A (u_2)_B} = 0$only.

The turbulence of isotropic is a model in a restricted domain, where it is not affected by the constraints encasing the fluid, also the measurable moments are orientation-independent and spatially invariant. The invariance condition under reflection in isotropic turbulence as regards to B is followed by,

$$\overline{(u_i)_B (u_k)_C (u_j)_C} = -\overline{(u_k)_B (u_j)_B (u_i)_C}$$

or, $(s_{i,kj})_{B,C} = -(s_{kj,i})_{B,C}$

Thus, Eq. (14) can be derived as

$$\frac{\partial}{\partial t} W_{i,j} - \frac{\partial}{\partial \tau_k}(S_{ik,j} + S_{kj,i}) = 2\upsilon \frac{\partial^2}{\partial \tau_k \partial \tau_k} W_{i,j} - 2\left[(M_{i,j} + N_{i,j}) + (F_{i,j} + G_{i,j})\sin\theta\right]$$

$$+\frac{\mu_f}{\rho}\left[-\frac{\partial}{\partial \tau_k}(D_{jk,i} + D_{ik,j}) + \frac{1}{3}\frac{\partial}{\partial \tau_k}(H_{ik,j} + H_{jk,i})\right] \tag{15}$$

The terms$\frac{\partial}{\partial \tau_k}(D_{jk,i} + D_{ik,j})$,$\frac{\partial}{\partial \tau_k}(S_{ik,j} + S_{kj,i})$,$\frac{\partial}{\partial \tau_k}(H_{ik,j} + H_{jk,i})$, $(M_{i,j} + N_{i,j})$, and $(F_{i,j} + G_{i,j})$ form second-order tensors, let denote these by$D_{i,j}$, $S_{i,j}$,$H_{i,j}$,$L_{i,j}$, and $Q_{i,j}$respectively and defined as:

$$D_{i,j} = \frac{\partial}{\partial \tau_k}(D_{jk,i} + D_{ik,j})\,S_{i,j} = \frac{\partial}{\partial \tau_k}(S_{ik,j} + S_{kj,i})$$

$H_{i,j} = \frac{\partial}{\partial \tau_k}(H_{ik,j} + H_{jk,i})$,$L_{i,j} = (M_{i,j} + N_{i,j})$, and $Q_{i,j} = (F_{i,j} + G_{i,j})$.

Therefore, Eq. (15) yields

$$\frac{\partial}{\partial t} W_{i,j} - S_{i,j} = 2\left[\upsilon \frac{\partial^2}{\partial \tau_k \partial \tau_k} W_{i,j} - L_{i,j} - Q_{i,j}\sin\theta\right] - \frac{\mu_f}{\rho}\left(D_{i,j} - \frac{1}{3} H_{i,j}\right) \tag{16}$$

This equation expresses the turbulent energy motion for fiber suspensions in the rotating system expressed in second-order correlation tensors.

Table 1 Equations of turbulent motion in terms of the pressure–velocity correlation tensors of second order.

Equations of turbulent motion	Consideration	References
$\frac{\partial}{\partial t}W_{i,j}-S_{i,j}=2\left[\upsilon\frac{\partial^2}{\partial\tau_k\partial\tau_k}W_{i,j}-L_{i,j}-Q_{i,j}\sin\theta\right]-\frac{\mu_f}{\rho}\left(D_{i,j}-\frac{1}{3}H_{i,j}\right)$	- turbulent energy motion- fiber suspensions- rotating frame	This study
$\frac{\partial}{\partial t}W_{i,j}-S_{i,j}=2\left[\upsilon\frac{\partial^2}{\partial\tau_k\partial\tau_k}W_{i,j}-L_{i,j}\right]-\frac{\mu_f}{\rho}\left(D_{i,j}-\frac{1}{3}H_{i,j}\right)$	- turbulent energy motion- fiber suspensions	Ahmed and Sarker [2]
$\frac{\partial}{\partial t}W_{i,j}-S_{i,j}=2\left[\upsilon\frac{\partial^2}{\partial\tau_k\partial\tau_k}W_{i,j}-L_{i,j}-Q_{i,j}\sin\theta\right]$	- turbulent energy motion- rotating frame	Ahmed [40]
$\frac{\partial}{\partial t}W_{i,j}-S_{i,j}=2\upsilon\frac{\partial^2}{\partial\tau_k\partial\tau_k}W_{i,j}$	- turbulent motion	Hinze [1]

3. Results and discussion

The particle dynamics in turbulent flows are a basic problem associated with the applications, for example, spray combustion engines, and atmospheric clouds. Suspensions of fiber in a gas or fluid have for some time been known to diminish the sharing stresses created as the fluid passes through a hard surface under turbulent flow conditions. The turbulent energy motion of the suspension of fibers (16) was obtained in a system of rotation. The equation was found in second-order velocity and pressure–velocity correlation tensors. All these tensors were formed as the function of distance, time, and space coordinates. Table 1 shows a comparison between the present and the existing similar type models.

Turbulent flows are broadly studied in the rotating system due to their extensive application in both engineering and geophysical fluid mechanics such as in blade passages of a gas turbine, nuclear reactor cores, rotary heat exchangers, rotary shafts, and combustion systems. In most of these engineering complications, a non-rotating (stationary coordinate) system is frequently used to analyze the problems. As mentioned earlier, the Coriolis force acts a vital role in a rotating system. For the non-rotating system, the Coriolis force does not generate in the flow field, which means$Q_{i,j}=0$, and thus the resulting Eq. (16) yields

$$\frac{\partial}{\partial t}W_{i,j}-S_{i,j}=2\left[\upsilon\frac{\partial^2}{\partial\tau_k\partial\tau_k}W_{i,j}-L_{i,j}\right]-\frac{\mu_f}{\rho}\left(D_{i,j}-\frac{1}{3}H_{i,j}\right) \quad (17)$$

The Eq. (17) represents the turbulent energy equation of fiber suspensions in second-order tensors which was obtained in the study of Ahmed and Sarker [2]. If fiber is not suspended into the flow domain, the viscosity (apparent) of the suspending fluid vanishes, which means,$\mu_f=0$, and therefore the Eq. (17) takes the form

$$\frac{\partial}{\partial t}W_{i,j}-S_{i,j}=2\left[\upsilon\frac{\partial^2}{\partial\tau_k\partial\tau_k}W_{i,j}-L_{i,j}\right] \quad (18)$$

Eq. (18) gives the energy motion of turbulent flow with correlation tensors [57].

Without any influence of energy dissipation by turbulence,$L_{i,j}=0$so that Eq. (18) becomes

$$\frac{\partial}{\partial t}W_{i,j}-S_{i,j}=2\upsilon\frac{\partial^2}{\partial\tau_k\partial\tau_k}W_{i,j} \quad (19)$$

Eq. (19) expresses the turbulent motion in the form of second-order correlation tensors that is similar to the study of Hinze [1].

4. Conclusion

In a rotating frame, the turbulent energy equation of fiber motion was derived in respect of velocity and pressure–velocity correlation tensors, where all the tensors are of second-order and the function of distance, space, and time coordinates. The turbulent flow of fiber suspensions undergoes random motion owing to the fluctuating components of fluid velocity, and average motion because of the average fluid velocity. The turbulent energy motion with fiber suspensions was obtained in a rotating frame by the averaging procedure. All the second-order tensors, $W_{i,j}, S_{i,j}, L_{i,j}, F_{i,j}, G_{i,j}, D_{i,j}, Q_{i,j}$and $H_{i,j}$found in the resulting Eq. (16) are the correlation tensors, where $W_{i,j}$and $S_{i,j}$ denote the velocity correlations, $D_{i,j}$and $H_{i,j}$signifies the velocity correlations for the suspending fluid, $L_{i,j}$designates the velocity correlations for turbulent energy at two points B and C of the flow field whereas $Q_{i,j}$expresses the correlation between the fluid particle velocity and angular velocity obtained because of the rotating frame. In our future work, the resulting Eq. (16) will be solved both numerically and analytically to assess the fiber suspension impact on turbulent flow in a rotating system which would contribute to science and industry, namely in papermaking, textile industry, chemical, and environmental engineering, and producing composite materials.

Declaration of Competing Interest

The authors declare that they have no known competing financial interests or personal relationships that could have appeared to influence the work reported in this paper.

Acknowledgments

The authors are grateful to the National Natural Science Foundation of China for their support in this research.

References

[1] J. Hinze, Turbulence McGraw-Hill Book Co, New York, (1959) 30-33.
[2] S.F. Ahmed, M.S.A. Sarker, Derivation of turbulent energy of fiber suspensions, Journal of Computational Applied Research in Mechanical, Engineering 4 (2015) 155–163.
[3] L. Jian-Zhong, L. Jun, Z. Li, J.A. Olson, New equation of turbulent fibre suspensions and its solution and application to the pipe flow, Chin. Phys. 14 (2005) 1185.

[4] S.F. Ahmed, M.S.A. Sarker, Fiber suspensions in turbulent flow with two-point correlation, Bangladesh Journal of Scientific and Industrial Research 46 (2011) 265–270.

[5] M.S.A. Sarker, S.F. Ahmed, Motion of fibres in turbulent flow in a rotating system, Rajshahi University Studies, Part-B, Journal of Science, (2009) 107-117.

[6] D. Dotto, C. Marchioli, Orientation, distribution, and deformation of inertial flexible fibers in turbulent channel flow, Acta Mech. 230 (2019) 597–621.

[7] A.A. Banaei, M. Rahmani, D.M. Martinez, L. Brandt, Inertial settling of flexible fiber suspensions, Phys. Rev. Fluids 5 (2020) 024301.

[8] D.O. Njobuenwu, M. Fairweather, Simulation of inertial fibre orientation in turbulent flow, Phys. Fluids 28 (2016) 063307.

[9] D. Oztekin, Z. Liu, C. Aidun, Computational simulation of fiber suspension in single and multiphase flow, Bulletin of the American Physical Society 63 (2018).

[10] Z. Ouyang, J. Lin, Y. Wang, F. Yuan, Fiber orientation distribution and rheological properties of fiber suspension in a turbulent jet, Korea-Australia Rheology Journal 30 (2018) 55–63.

[11] W. Lin, S. Sun, F. Yuan, S. Shen, Numerical simulation and visualization of fiber suspension in a turbulent round jet, Appl. Math. Mech. 38 (2017) 1651–1662.

[12] Y. Xia, X.-K. Ku, S.-H. Shen, Flow property of fiber suspension in a turbulent channel flow under considering both Brownian and turbulent diffusions, Acta Physica Sinica 65 (2016) 194702.

[13] N.R. Challabotla, L. Zhao, H.I. Andersson, On fiber behavior in turbulent vertical channel flow, Chem. Eng. Sci. 153 (2016) 75–86.

[14] N.R. Challabotla, L. Zhao, H.I. Andersson, Gravity effects on fiber dynamics in wall turbulence, Flow, Turbulence and Combustion 97 (2016) 1095–1110.

[15] C. Marchioli, L. Zhao, H. Andersson, On the relative rotational motion between rigid fibers and fluid in turbulent channel flow, Phys. Fluids 28 (2016) 013301.

[16] D. Dotto, A. Soldati, C. Marchioli, Deformation of flexible fibers in turbulent channel flow, Meccanica 55 (2020) 343–356.

[17] S.F. Ahmed, M.G. Hafez, Y.-M. Chu, Conversion of energy equation for fiber suspensions in dusty fluid turbulent flow, Results Phys. 19 (2020) 103341.

[18] H. Cho, J. Iribarne, W. Richards, On the orientation of ice crystals in a cumulonimbus cloud, J. Atmos. Sci. 38 (1981) 1111–1114.

[19] B. Asgharian, C. Yu, Deposition of fibers in the rat lung, J. Aerosol Sci. 20 (1989) 355–366.

[20] M. Belka, F. Lizal, J. Jedelsky, J. Elcner, P.K. Hopke, M. Jicha, Deposition of glass fibers in a physically realistic replica of the human respiratory tract, J. Aerosol Sci. 117 (2018) 149–163.

[21] O. Bernstein, M. Shapiro, Direct determination of the orientation distribution function of cylindrical particles immersed in laminar and turbulent shear flows, J. Aerosol Sci. 25 (1994) 113–136.

[22] J. Lin, X. Shi, Z. Yu, The motion of fibers in an evolving mixing layer, Int. J. Multiph. Flow 29 (2003) 1355–1372.

[23] L. Jianzhong, Z. Weifeng, Y. Zhaosheng, Numerical research on the orientation distribution of fibers immersed in laminar and turbulent pipe flows, J. Aerosol Sci. 35 (2004) 63–82.

[24] H. Kagermann, W. Koehler, On the motion of nonspherical particles in a turbulent flow, Physica A 116 (1982) 178–198.

[25] J.A. Olson, The motion of fibres in turbulent flow, stochastic simulation of isotropic homogeneous turbulence, Int. J. Multiph. Flow 27 (2001) 2083–2103.

[26] Z.-Y. Gao, J.-Z. Lin, Dispersion of cylindrical particles in turbulent flows, JOURNAL OF HYDRODYNAMICS SERIES B-ENGLISH EDITION- 16 (2004) 1–6.

[27] L. Jian-zhong, L. Jiang, S. Xing, Research on the effect of cylinder particles on the turbulent properties in particulate flows, Appl. Math. Mech. 23 (2002) 542–548.

[28] W. Yang, K. Zhou, Z.-L. Zhao, Z.-H. Wan, Study on the two-way coupling turbulent model and rheological properties for fiber suspension in the contraction, J. Nonnewton. Fluid Mech. 246 (2017) 1–9.

[29] S.M. Ahmed, S.N. Kazi, G. Khan, N. Akram, M. Dahari, M.N. M. Zubir, P. Ahmad, T. Zaharinie, Experimental investigation on drag reduction of flowing crop suspensions of the pulp fibers in circular pipe heat exchanger, Part. Sci. Technol. (2019).

[30] S. Ahmed, S. Kazi, G. Khan, M. Dahari, M. Zubir, P. Ahmad, E. Montazer, Experimental investigation on momentum and drag reduction of Malaysian crop suspensions in closed conduit flow, in: IOP Conference Series: Materials Science and Engineering, 2017, pp. 012065.

[31] F. Rashid, H.N. Azziz, S.M. Talib, Experimental Investigation of Drag Reduction by a Polymeric Additive in Crude Oil Flow in Horizontal Pipe, Journal of Advanced Research in Fluid Mechanics and Thermal Sciences 60 (2019) 15–23.

[32] S.F. Ahmed, Turbulent energy for dusty fluid in a rotating system, International, J. Appl. Math. Mech. 9 (2013) 50–61.

[33] R. Kristoffersen, H.I. Andersson, Direct simulations of low-Reynolds-number turbulent flow in a rotating channel, J. Fluid Mech. 256 (1993) 163–197.

[34] S. Akar, S. Rashidi, J.A. Esfahani, Second law of thermodynamic analysis for nanofluid turbulent flow around a rotating cylinder, J. Therm. Anal. Calorim. 132 (2018) 1189–1200.

[35] M. Murakami, K. Kikuyama, Turbulent flow in axially rotating pipes, (1980).

[36] H. You, H. Li, R. You, Z. Tao, J. Shi, Experimental Investigations of Turbulent Flow in a Rotating Ribbed Channel in Terms of the Effect of Coriolis Force, in: Turbo Expo: Power for Land, Sea, and Air, American Society of Mechanical Engineers, 2019, pp. V05AT16A004.

[37] Q.-Q. Xun, B.-C. Wang, Hybrid RANS/LES of turbulent flow in a rotating rib-roughened channel, Phys. Fluids 28 (2016) 075101.

[38] M. Rosales, T. Pérez, J.L. Nava, Computational fluid dynamic simulations of turbulent flow in a rotating cylinder electrode reactor in continuous mode of operation, Electrochim. Acta 194 (2016) 338–345.

[39] A.A. Avramenko, I.V. Shevchuk, A.V. Kravchuk, Turbulent incompressible microflow between rotating parallel plates, European Journal of Mechanics-B/Fluids 71 (2018) 35–46.

[40] S.F. Ahmed, Derivation of turbulent energy in a rotating system, Journal of Computational & Applied Research in Mechanical Engineering (JCARME) 3 (2013) 75–83.

[41] I. Mahariq, M. Kavyanpoor, M. Ghalandari, M.A. Nazari, D. T. Bui, Identification of nonlinear model for rotary high aspect ratio flexible blade using free vibration response, Alexandria Engineering Journal (2020).

[42] T. Abdeljawad, I. Mahariq, M. Kavyanpoor, M. Ghalandari, N. Nabipour, Identification of nonlinear normal modes for a highly flexible beam, Alexandria Engineering Journal (2020).

[43] C.G. Speziale, S. Sarkar, T.B. Gatski, Modelling the pressure–strain correlation of turbulence: an invariant dynamical systems approach, J. Fluid Mech. 227 (1991) 245–272.

[44] S.F. Ahmed, M.S.A. Sarker, Fiber Motion in Dusty Fluid Turbulent Flow in a Rotating System, International Journal of Applied Mathematics and Mechanics 10 (2014) 92–109.

[45] R. You, H. Li, Z. Tao, K. Wei, G. Xu, PIV measurements of turbulent flows in a smooth channel with the heated boundary under rotation conditions, Appl. Therm. Eng. 123 (2017) 1021–1033.

[46] M. Al-Smadi, O.A. Arqub, S. Hadid, An attractive analytical technique for coupled system of fractional partial differential equations in shallow water waves with conformable derivative, Commun. Theor. Phys. 72 (2020) 085001.

[47] M. Al-Smadi, O.A. Arqub, S. Hadid, Approximate solutions of nonlinear fractional Kundu-Eckhaus and coupled fractional massive Thirring equations emerging in quantum field theory using conformable residual power series method, Phys. Scr. 95 (2020) 105205.

[48] M. Al-Smadi, O.A. Arqub, Computational algorithm for solving fredholm time-fractional partial integrodifferential equations of dirichlet functions type with error estimates, Appl. Math. Comput. 342 (2019) 280–294.

[49] M. Alabedalhadi, M. Al-Smadi, S. Al-Omari, D. Baleanu, S. Momani, Structure of optical soliton solution for nonliear resonant space-time Schrödinger equation in conformable sense with full nonlinearity term, Phys. Scr. 95 (2020) 105215.

[50] I. Mahariq, A. Erciyas, A spectral element method for the solution of magnetostatic fields, Turkish Journal of Electrical Engineering & Computer Sciences 25 (2017) 2922–2932.

[51] I. Mahariq, H. Kurt, M. Kuzuoğlu, Questioning degree of accuracy offered by the spectral element method in computational electromagnetics, Appl. Comput. Electromagnet. Soc. J. 30 (2015) 698–705.

[52] I. Mahariq, On the application of the spectral element method in electromagnetic problems involving domain decomposition, Turkish Journal of Electrical Engineering & Computer Sciences 25 (2017) 1059–1069.

[53] I. Mahariq, M. Kuzuoğlu, I.H. Tarman, H. Kurt, Photonic nanojet analysis by spectral element method, IEEE Photonics J. 6 (2014) 1–14.

[54] I. Mahariq, M. Kuzuoğlu, I.H. Tarman, On the Attenuation of the Perfectly Matched Layer in Electromagnetic Scattering Problems with the Spectral Element Method, Applied Computational Electromagnetics Society Journal 29 (2014).

[55] I. Mahariq, H. Kurt, Strong field enhancement of resonance modes in dielectric microcylinders, JOSA B 33 (2016) 656–662.

[56] I. Mahariq, H. Tarman, M. Kuzuoğlu, On the accuracy of spectral element method in electromagnetic scattering problems, Int. J. Comput. Theory Eng 6 (2014) 495–499.

[57] S.F. Ahmed, Derivation of energy equation for turbulent flow with two-point correlation, Pure and Applied Mathematics Journal 2 (2013) 197–200.